

This is a postprint version of the following published document:

Algorri, José Francisco; García-Cámara, Braulio; Cuadrado Conde, Alexander; Sánchez-Pena, José Manuel; Vergaz Benito, Ricardo (2016). Optimized Minimum-Forward Light Scattering by Dielectric Nanopillars. *IEEE Photonics Technology Letters*, 28(20), pp.: 2160-2163.

DOI: <https://doi.org/10.1109/LPT.2016.2585678>

©2020 IEEE. Personal use of this material is permitted. Permission from IEEE must be obtained for all other uses, in any current or future media, including reprinting/republishing this material for advertising or promotional purposes, creating new collective works, for resale or redistribution to servers or lists, or reuse of any copyrighted component of this work in other works.

See <https://www.ieee.org/publications/rights/index.html> for more information.

Optimized Minimum-Forward Light Scattering by dielectric nanopillars

José Francisco Algorri, Braulio García-Cámara, Alexander Cuadrado Conde, José Manuel Sánchez-Pena, *Senior Member, IEEE*, Ricardo Vergaz Benito

Abstract— In this study, silicon nanopillars with an optimum aspect ratio are analyzed, in such a way that the overlapping of the electric and magnetic dipolar resonances provides a remarkable minimum forward scattering. This ideal shape is also related with the incident wavelength and the refractive index of the surrounding medium. We work in the frame of numerical simulations based on Maxwell equations solved by the Finite Element Method. When the aspect ratio implies a nanopillar, a linear behavior for the minimum forward condition is observed. An upper limit of the aspect ratio has been found to satisfy the minimum forward condition. This aspect ratio is determinant in order to scale these systems with wavelength. A larger efficiency at the directional conditions is also shown with respect to silicon nanodisks. These results are promising for design and create novel CMOS integrated flat optical devices.

Index Terms—Nanophotonics, Nanoparticles, Resonance light scattering, Silicon photonics.

I. INTRODUCTION

The International Roadmap for Devices and Systems (ITRS) has formally acknowledged that Moore's law is nearing its end [1]. Moreover, the speed clock in CPUs reached their practical limit in 2004. One of the main problems is the heat caused by the movement of electrons. For these reasons, it is time to find other solutions that could get beyond Moore's law. Several research groups are actively working on the design of photonic circuits [2]. All optical devices may be the best solution to replace the tracks within the chips, changing into optical circuitry, and increase the speed limit, reducing the size. One of the main requirements in order to control the light in such small dimensions would be the control of light scattering at the nanoscale.

This work has been supported by Ministerio de Economía y Competitividad of Spain (grants no. TEC2013-47342-C2-2-R and no.TEC2013-50138-EXP) and the R&D Program SINFOTON S2013/MIT-2790 of the Comunidad de Madrid.

J. F. Algorri, B. García-Cámara, J. M. Sánchez-Pena and R. Vergaz Benito are with the Electronic Technology Department, Carlos III University of Madrid, E-28911 Leganés, Madrid. (Corresponding author phone: 0034916245964; fax: 0034916249430; e-mail: brgarcia@ing.uc3m.es, jalgorri@ing.uc3m.es, jmpena@ing.uc3m.es, rvergaz@ing.uc3m.es).

A. Cuadrado Conde is with Laser Processing Group, Instituto de Óptica, CSIC, C/Serrano 121, 28006 Madrid, Spain (email: a.cuadradoconde@gmail.com)

Kerker's conditions were theoretically proposed for spherical particles in 1983 [3]. Two conditions were predicted; the first condition states that a zero-backscattering (ZB) can be achieved. When the second one is satisfied, a destructive interference in the forward direction is produced while light scattering is concentrated in the backward direction (zero forward, ZF). The theoretical work of Kerker was experimentally demonstrated at micrometric wavelengths in 2012 [4] and at nanometric wavelengths in 2013 [5, 6]. In these works, it was shown that semiconductor nanoparticles, like Silicon or Germanium, present both electric and magnetic resonances, interacting as it was predicted by Kerker et al. Despite the results of Kerker, several works have shown that zero-forward scattering cannot be achieved, and only a minimum forward (MF) scattering can be obtained [7]. These resonances behave like plasmon ones, depending on the size, shape and the optical properties of the surrounding medium [8]. Thus, the observation of the directional phenomena can be controlled by changing these parameters. In addition, a significant great overlap of the electric and magnetic dipolar resonances, and in consequence a remarkable MF scattering, can be realized if spheroids [9] and disks [10] are considered. In recent years also the scattering properties of nanorods have been engineered by integrating "tapered" or "coned" structures into the nanoparticle [11, 12]. Also the scattering in nanopillars [13] and needles [14] has been investigated.

In this work, an optimum MF scattering is found for silicon nanopillars with convenient aspect ratio. Several parameters are taken into account, like the aspect ratio, the incident wavelength and the underlying substrate. These results could be determinant to use the proposed designs in practical devices with fabrication feasibility. Besides, they have an almost negligible optical and thermal absorption and have the advantage of compatibility with current CMOS techniques. Consequently, they are ideal candidates to be used in integrated CMOS nanoelectronic devices as optical counterparts.

II. ABSORPTION AND SCATTERING IN SI NANOPILLARS

Our framework is a set of numerical simulations based on Maxwell equations solved by finite element method (COMSOL®). A plane TE-polarized electromagnetic wave is normally incident on a silicon nanopillar (NP) embedded in air. The absorption (Eq. 1) and scattering (Eq. 2) cross sections [11] of the NP can be expressed as

$$\sigma_{abs} = \frac{1}{I_0} \iiint Q dV \quad (1)$$

$$\sigma_{sc} = \frac{1}{I_0} \iint (\mathbf{n} \cdot \mathbf{S}_{sc}) dS \quad (2)$$

where Q is the power loss density in the NP. \mathbf{n} is the normal vector pointing outwards from the nanoparticle. \mathbf{S}_{sc} is the scattered intensity (Poynting) vector, and I_0 is the incident intensity. While for the case of the absorption, the integral is taken over the volume of the nanoparticles, in the second case it is taken over the surface of the scatterer. The extinction (Eq. 3) cross section can be estimated by the sum of previous ones.

$$\sigma_{ext} = \sigma_{abs} + \sigma_{sc} \quad (3)$$

In this work the goal is to detect the best configuration in which a MF scattering is obtained, and to determine the dependence of it with the dimensional and wavelength parameters. Several height, radius and incident wavelengths are considered in our simulations. The range of particle sizes were chosen in such a way that the directional behaviors appear in the visible and near-infrared ranges, in which photonic applications are currently being developed.

Figure 1 is an example of the extinction and absorption cross sections that can be obtained for nanoparticles embedded in air, as their radius (R) changes for a certain combination of their height ($H = 160$ nm in this case) and the incident light wavelength ($\lambda = 632.8$ nm in this case). An inset with the structure and these mentioned parameters is included within the figure. As it can be seen, absorption cross section is more than one order of magnitude lower than scattering, thus hereinafter the discussion will be focused only on scattering cross section. As we have demonstrated in previous works, certain intersections between electric and magnetic dipolar contributions produce MF conditions [3, 8]. These intersections are mainly located between peaks at the cross section plots. The local minima are unveiling the points where MF Kerker's condition is satisfied. Fig. 1 shows two such

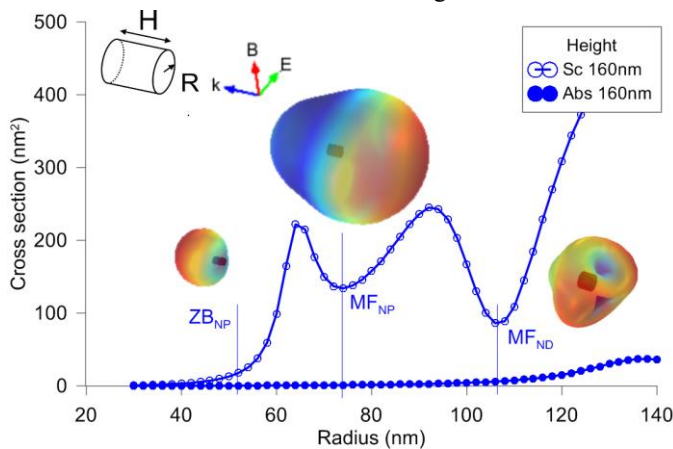


Fig. 1. Absorption and scattering cross section (nm^2) of a nanoparticle of height $H = 160$ nm, illuminated with a beam with a wavelength $\lambda = 632.8$ nm as a function of radius. Vertical lines indicating radii at which ZB, MF of a nanopillar and MF of a nanodisk are obtained. The inset shows the NP structure and the direction of the incidence light (\mathbf{k}).

minima, with different aspect ratios (defined as $\mathcal{R} = H/2R$). One of them is found at smaller radius, $R = 74$ nm, in which the nanoparticle resembles a NP. The other one is found at a radius $R = 106$ nm, for which the nanoparticle is geometrically a nanodisk (ND). The far-field FEM simulation (calculated from the near-field on a boundary using Stratton-Chu formula, units are in V/m) is shown, as insets, for each one of these points, showing the effect of minimum scattering towards the forward direction (light impinges in the \mathbf{k} vector direction). There is another interesting point marked on the left of the graph, where a ZB condition is obtained for small radius, $R = 52$ nm, as it can be seen in the FEM simulation graph. While the ZB condition produces a deep lack of scattered field in the backward direction, the MF condition produces a noticeable reduction of forward scattering, but not zero. These results are focused in the He-Ne laser wavelength to facilitate experimental verification. Nevertheless, a combination of certain wavelength, radius and height would produce a minimum value for all the local minima found in the scattering cross-section for NPs and NDs. In that case, an optimum condition could be found.

The first relevant feature of Figure 1 is that we can find two radii for the same height that lead to a minimum forward condition. The next step is the detection of these two radii for every combination of wavelength and height. For the sake of clarity, only four wavelengths are plotted in Figure 2: $\lambda = 632.8, 800, 1000$ and 1250 nm, to show in a single plot the trend of the dependence of the height where the MF condition is found as a function of radius. As it can be seen, the condition is not found for every height, and its appearance is

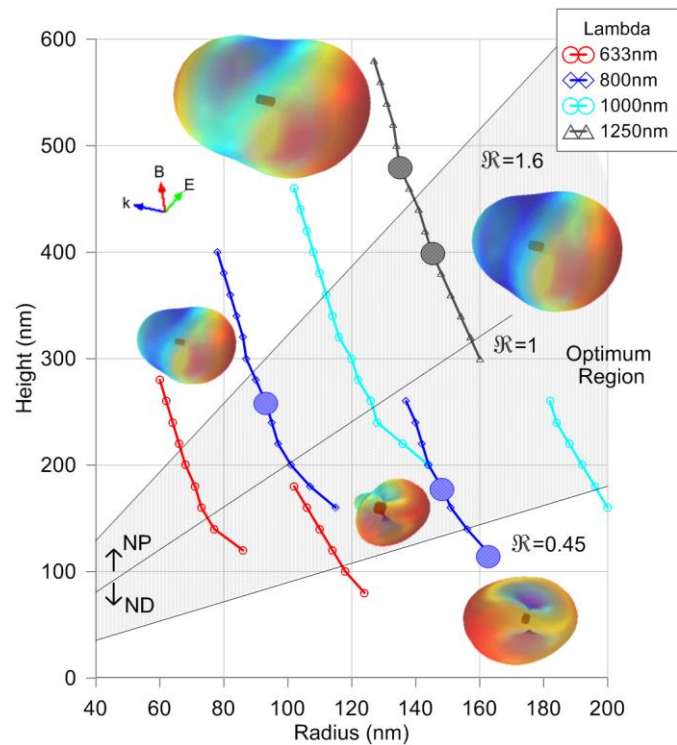


Fig. 2. Relation between the height and the radius of silicon nanoparticles satisfying the minimum forward scattering conditions at different incident wavelengths. Optimum observation regions are delimited and shadowed. Also, some spatial distributions of the scattered far field at five different remarked points are included.

strongly linked with the aspect ratio. Thus, as the wavelength increases, the conditions appear with larger dimensions. Moreover, there are two branches for each wavelength, which spreads into two regions of aspect ratios \mathfrak{R} (shaded between straight lines in Fig. 2). Although, we found H - R combinations satisfying the MF conditions out of these regions, the spatial distribution of the scattered fields (see insets of Fig. 2) do not resemble the typical MF distribution, as those observed in these regions. The first optimum region, between $\mathfrak{R} = 1.6$ and $\mathfrak{R} = 1$, corresponds to NPs, and the second one is between $\mathfrak{R} = 1$ and $\mathfrak{R} = 0.45$, with ND geometries. The MF pairs show linear trends between height and radius into these regions. We guess that this linear result could be related with the behavior of the electric and magnetic dipolar resonances that are coherently interfering to create the directional conditions. While the magnetic dipolar resonance stands still as radius increases, the electric resonance follows a linear trend according Fröhlich theory [15].

Insets of Fig. 2 show representative examples (remarked points) of far field scattering of each one of these regions. The comparison between them shows an evident different behavior. While in the case of the NP (upper optimum region at Fig. 2) the profile is as expected, with a low intensity in the forward direction, the scattering profile of the ND (bottom optimum region at Fig. 2) is more complex. As it was previously commented, points out of the above described two regions loose the far field scattering distribution with respect the MF condition. As an example, when the aspect ratio, defined as $\mathfrak{R} = H/2R$, is higher than 1.6 (e.g. Fig 3, $\lambda = 1250\text{nm}$, $H = 480\text{nm}$, $R = 135\text{nm}$), the NP begins to spread the light also in the forward direction. This effect is also observed for aspect ratios lower than 0.45 (e.g. Fig 3, $\lambda = 800\text{nm}$, $H = 120\text{nm}$, $R = 162\text{nm}$). This, limits the appearance of the MF condition to both optimum regions.

Analyzing Fig. 2, it can be deduced that for a certain height

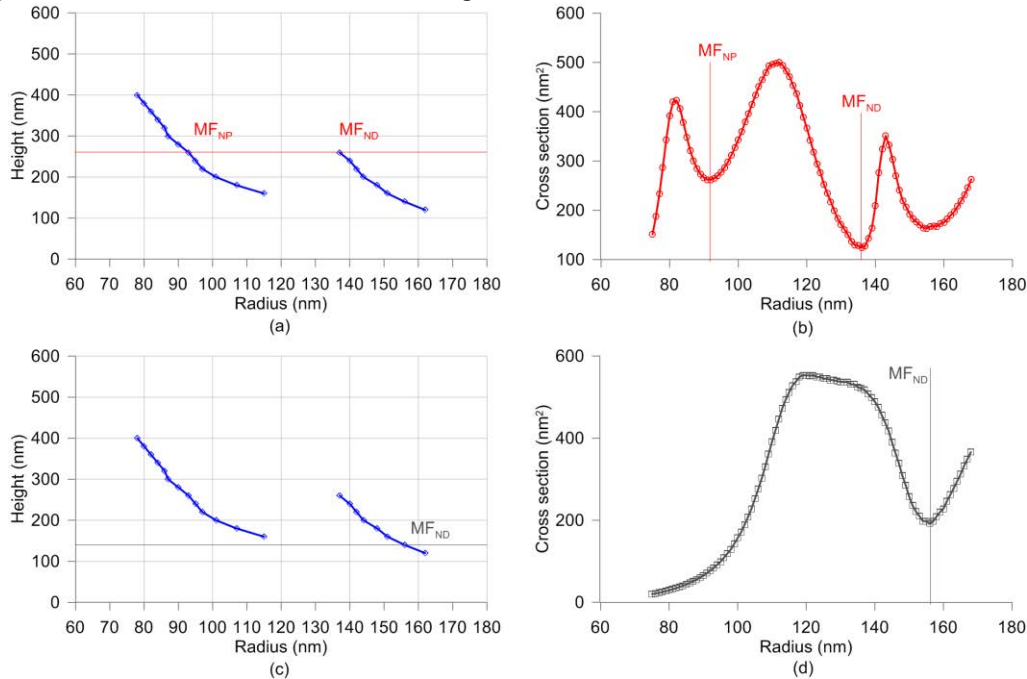


Fig. 3. Relation of the pairs height-radius of a nanoparticle satisfying the MF conditions at an incident wavelength of $\lambda = 800\text{nm}$, remarking with a horizontal line the crosses of (a) $H = 260\text{nm}$ and (c) $H = 140\text{nm}$. The scattering cross section of the nanoparticle with the considered heights are plotted in (b) and (d), respectively. The previous intersection points are now remarked as vertical lines.

of the nanoparticle, one or two radius can lead to MF condition at the same incident wavelength, one corresponding to a NP geometry and the other one to a ND. Fig. 3 shows two representative examples for $\lambda = 800\text{nm}$ and two different heights. For the first one, $H = 260\text{nm}$, two radius can be detected where MF condition is achieved, (Fig. 3a). The corresponding scattering cross section versus radius of the considered nanoparticle is shown in Fig. 3b. The previous radii are remarked as vertical lines. Certainly, they both correspond with local minima, one for $R = 90\text{nm}$ and the other one for $R = 136\text{nm}$; a NP and a ND shape, respectively. Although the scattering profiles are expected to be similar in both cases, the scattering cross section of the NP is 134nm^2 , and the ND is only 86.1nm^2 . This feature is general for all the MF cases: NPs scatter more efficiently than NDs.

Moreover, for the second height, $H = 140\text{nm}$, only one intersection can be found and it belongs to the ND region. Correspondingly only one local minimum is found in the cross section versus radius plot, at $R = 156\text{nm}$. This point is represented in the insets of Fig. 2 showing a complex scattering profile.

Both NPs and NDs are convenient geometries due to its easy fabrication. However, these results show that, although a MF scattering can be observed in both cases, NPs have a larger scattering cross section than NDs at that condition, even considering that the size of the NDs dimension intersecting the light is bigger. In addition, in the case of NPs the scattering distribution is similar than spherical nanoparticles, with a high concentration of light in the backward direction. We have found a linear relation between the height and the radius of the NP satisfying the MF conditions, as well as the scalability of this condition with the wavelength in terms of size dimensions. In particular, the last statement could be very interesting for the extrapolation of these phenomena far beyond the infrared spectrum (GHz, THz, etc.). This idea has

to be further investigated because it could open new possibilities for the easy design of new devices at this spectrum range.

III. SUBSTRATE INFLUENCE

One of the main obstacles to observe this directional phenomenon as clearly as possible is related to the substrate effect. Figure 4 shows the far field for three NPs arranged over different substrates. The size of the NPs is one of the previously analyzed, in particular $H = 160$ nm and $R = 72$ nm, and the light impinges over the substrate in the \mathbf{k} direction of its normal, with $\lambda = 632.8$ nm (MF_{NP} at Fig. 1). (In the supplementary information, a sweep over the radius is performed in three different videos corresponding to Fig.4 (a), Fig.4 (b) and Fig.4 (c)). As the change of refractive index only occurs in a small surface of the nanoparticle, the condition is satisfied for the same size and wavelength. As it is demonstrated in Fig.4 (a), when an ultra-low refractive index substrate is used (e.g. Aerogel, $n = 1.032$ at 632nm), the MF scattering condition remains unaltered. At an intermediate case, (Magnesium Fluoride, MgF₂, $n = 1.377$ at 632nm, Fig. 4b) the profile of the scattering cannot show a predominant direction, and the field is located both in the forward and backward directions. If the refractive index of the substrate increases even more, we can see that, in spite of the fulfillment of the MF condition, scattered light is mainly concentrated in the forward direction. This is shown in Fig 4 (c), where a substrate with refractive index around 1.8-2 (Alumina, Al₂O₃, $n = 1.766$ at 632nm) is considered. As can be seen, most part of the scattering is deviated through the substrate, while the backscattering is reduced.

These results reveal that the use of substrates with low refractive index is required in order to exploit the above described effect. Another solution could be the arrangement in meta-surfaces that could reduce the overall substrate effect. Subwavelength-scaled patterns in 2D dimensions could reduce the amount of light impinging on the substrate and in consequence the effect of the same one. Any of these two possibilities would allow the use of the proposed designs.

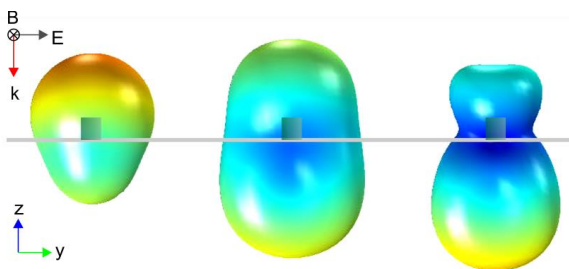


Fig. 4. Far field scattering for $\lambda = 632.8$ nm, $H = 160$ nm, $R = 72$ nm and different substrates, (a) Aerogel, (b) MgF₂ and (c) Al₂O₃.

IV. CONCLUSIONS

As a summary, we numerically analyzed the size, wavelength and substrate dependence of the MF-scattering

condition in silicon NPs. We have obtained several interesting results. The scattering cross section analysis reveals that the use of silicon NPs is more convenient than NDs concerning the observance of minimum forward scattering. Even more, NDs produce sharp minima in the scattering cross sections, which reduces their manufacturing tolerance to achieve a MF condition. An optimum region for the MF condition is determined by the aspect ratio of the NP. This would be determinant in order to scale these systems with wavelength. A linear trend for the MF condition of the height with increasing radius dependent on radius to height ratio is demonstrated. Finally, several substrates are studied as supports for the NPs. In conclusion, the use of low index substrates or meta-surface arrangements could lead to the use of the proposed designs in practical devices.

REFERENCES

- [1] M. M. Waldrop, The chips are down for Moore's law, *Nature* 530, 144–147, 11 February 2016.
- [2] P. P. Absil, P. Verheyen, P. D. Heyn, M. Pantouvaki, G. Lepage, J. D. Coster, J. V. Campenhout, "Silicon photonics integrated circuits: a manufacturing platform for high density, low power optical I/O's," *Opt. Express*, vol. 23, pp. 9369-9378, 2015.
- [3] M. Kerker, D. S. Wang, C. L. Giles, "Electromagnetic scattering by magnetic spheres" *J. Opt. Soc. Am.*, vol. 73, pp. 765-767, 1983.
- [4] Geffrin, J.M., et al., "Magnetic and electric coherence in forward- and back-scattered electromagnetic waves by a single dielectric subwavelength sphere" *Nature Commun.*, vol. 3, 1171, 2012.
- [5] Y. H. Fu, A.I. Kutnetsov, A.E. Miroshnichenko, Y.F. Yu and B. Luk'yanchuk, "Directional visible light scattering by silicon nanoparticles" *Nat. Commun.*, vol. 4, 1527, Feb. 2013.
- [6] S. Person, M. Jain, Z. Lapin, J.J. Sáenz, G. Wicks, and L. Novotny, "Demonstration of Zero Optical Backscattering from Single Nanoparticles," *Nano Lett.*, vol. 13, no. 4, pp. 1806-1809, Mar. 2013.
- [7] R. Gómez-Medina, B. García-Cámara, I. Suarez-Lacalle, F. González, F. Moreno, M. Nieto-Vesperinas and J.J. Sáenz, "Electric and magnetic dipolar response of germanium nanospheres: interference effects, scattering anisotropy, and optical forces," *J. Nanophoton.*, vol. 5, no.1, 053512, Jun. 2011.
- [8] B. García-Cámara, J. F. Algorri, A. Cuadrado, V. Urruchi, J. M. Sánchez-Pena, R. Vergaz, "Size dependence of the directional scattering conditions on resonant semiconductor nanoparticles", *IEEE Photon. Technol. Lett.*, vol. 27, no. 19, pp. 2059-2062, 2015.
- [9] Boris S. Luk'yanchuk, Nikolai V. Voshchinnikov, Ramón Paniagua-Domínguez, and Arseniy I. Kuznetsov, "Optimum Forward Light Scattering by Spherical and Spheroidal Dielectric Nanoparticles with High Refractive Index" *ACS Photonics*, vol. 2, no. 7, pp. 993-999, 2015.
- [10] I. Staude, A. E. Miroshnichenko, M. Decker, N. T. Fofang, S. Liu, E. Gonzales, J. Dominguez, T. S. Luk, D. N. Neshev, I. Brener, Y. S. Kivshar, "Tailoring Directional Scattering through Magnetic and Electric Resonances in Subwavelength Silicon Nanodisks," *ACS Nano*, vol 7, no. 9, pp. 7824-7832, 2013.
- [11] X-L. Chu, T. J. K. Brenner, X-W. Chen, Y. Ghosh, J. A. Hollingsworth, V. Sandoghdar, and S. Götzinger. "Experimental realization of an optical antenna designed for collecting 99% of photons from a quantum emitter." *Optica* vol. 1, no. 4, pp. 203-208, 2014.
- [12] S. Xie, R. Pennetta, and P. St.J. Russell, "Self-alignment of glass fiber nanopike by optomechanical back-action in hollow-core photonic crystal fiber", *Optica*, vol. 3, no. 3, pp. 277-282, 2016.
- [13] P. Ding, M. Li, J. He, J. Wang, C. Fan, F. Zeng, "Guided mode caused by silicon nanopillar array for light emission enhancement in color-converting LED," *Opt. Express*, vol. 23, pp. 21477-21489, 2015.
- [14] R. Schiffer, K. O. Thielheim, "Light scattering by dielectric needles and disks," *J. of App. Physics*, vol. 50, pp. 2476-2483, 1979.
- [15] C.F. Bohren, and D.R. Huffman, *Absorption and Scattering of Light by Small Particles*, Weinheim: Wiley-VCH Verlag GmbH, 1983.